Title

Propagation Dynamics Associated with Resonant Magnetic Perturbation Fields in High-Confinement Mode Plasmas inside the KSTAR Tokamak

Journal

Physical Review Letters, 119(20)

ISSN

0031-9007

Authors

Xiao, WW
Evans, TE
Tynan, GR
et al.

Publication Date

2017-11-17

DOI

10.1103/physrevlett.119.205001

Peer reviewed

Propagation Dynamics Associated with Resonant Magnetic Perturbation Fields in High-Confinement Mode Plasmas inside the KSTAR Tokamak

W. W. Xiao,[1] T. E. Evans,[2] G. R. Tynan,[3] S. W. Yoon,[4] Y. M. Jeon,[4] W. H. Ko,[4] Y. U. Nam,[4] Y. K. Oh[4] and KSTAR team

[1]*Institute for Fusion Theory and Simulation, Zhejiang University, Hangzhou 310027, China*
[2]*General Atomics, P.O. Box 85608, San Diego, California 92186–5608, USA*
[3]*Center for Energy Research, University of California San Diego, La Jolla, California 92093, USA*
[4]*National Fusion Research Institute, Gwahango, 113, Daejeon, 305-333, Korea*

(Received 18 April 2017; revised manuscript received 4 September 2017; published 15 November 2017)

The propagation dynamics of resonant magnetic perturbation fields in KSTAR H-mode plasmas with injection of small edge perturbations produced by a supersonic molecular beam injection is reported for the first time. The results show that the perturbation field first excites a plasma response on the $q = 3$ magnetic surface and then propagates inward to the $q = 2$ surface with a radially averaged propagation velocity of resonant magnetic perturbations field equal to 32.5 m/ s. As a result, the perturbation field brakes the toroidal rotation on the $q = 3$ surface first causing a momentum transport perturbation that propagates both inward and outward. A higher density fluctuation level is observed. The propagation velocity of the resonant magnetic perturbations field is larger than the radial propagation velocity of the perturbation in the toroidal rotation.

DOI: 10.1103/PhysRevLett.119.205001

Transport in stochastic systems is an important branch of research that crosses a wide range of physics disciplines including dynamical systems theory [1,2], fluid dynamics [3], as well as space, solar, and astrophysics [4]. In magnetically confined plasmas, applied resonant magnetic perturbation (RMP) fields can cause stochasticity and transport [5]. Here, we report the first investigations of the propagation dynamics of resonant magnetic perturbations (RMPs) fields in KSTAR H-mode plasmas using injection of small edge perturbations produced by a supersonic molecular beam injection (SMBI) system. We show that the plasma response to the $n = 1$ RMP on $q_{95} \sim 5.0$ KSTAR H-mode plasmas is initially localized at the $q = 3$ rational surface, where a resonant tearing mode is predicted to be unstable, and then the response to the RMP field is subsequently observed at the $q = 2$ rational surface with a time delay, demonstrating the propagating of the RMP field in the plasma. In addition, we also show that the plasma response to the RMP field results in a modification of plasma turbulence. These results provide a new understanding of how RMP fields can affect magnetic tearing and stochasticity on specific rational surfaces as well as the subsequent impact of the modified magnetic topology on the plasma turbulence and transport. RMP fields have been successfully used to control edge-localized modes (ELMs) [6] and will be used in the international thermonuclear experimental reactor (ITER) [7] in order to avoid large energy transients on the divertor produced by type-I ELMs. The mechanism of RMP control of ELMs, as originally suggested by the first experiments [6], assumed the control of the pedestal pressure with the help of an enhanced transport in the stochastic magnetic field region formed by externally applied RMPs. Subsequently, an analysis using a linear kinetic model of RMP penetration into a plasma was developed in [8] and a quasilinear model was introduced [9]. However, the direct measurement of RMP propagation in magnetically confined plasmas has not been reported yet, and there are only indirect observations of how far and how quickly the RMP penetrates into plasma [10,11].

In this Letter, to probe the propagation of the RMP fields in plasma, we actively induce perturbations in the plasma response by applying small edge plasma perturbations with a train of pulsed supersonic molecular beam injections [12] during a steady state RMP. The use of modulated SMBI provides a time varying perturbation to both the plasma density source in the region just inside the last closed flux surface (via modulation of the neutral density) and a modulated flow damping rate (via ion-neutral charge exchange and elastic scattering). The resulting periodic perturbations then allow application of transient transport analysis techniques to determine the location of the first resonant plasma response to the RMP field. Such perturbations in the plasma response to RMP can be observed by measuring the resulting changes in the plasma toroidal rotation and thus the propagation of the change in plasma response to RMP can be directly measured. The radial phase of the perturbed toroidal rotation velocity (δv_ϕ) has two minima located at the $q = 2$ and 3 rational surfaces, respectively. The two phase minima represent the location of the fist and the second plasma response to RMP since the formation

of a phase minima is usually due to the presence of source term [13] and in this case, due to the perturbed RMP braking term in the toroidal momentum balance equation. The radial averaged propagation velocity of the RMP (V_{RMPP}) between the two rational surfaces can be thus inferred from the phase difference between the two minima since such a phase difference represents a time delay. We also show that the perturbed momentum transport during application of the RMP is both inward and outward from the $q = 3$ surface. In addition, the radial correlation length of the density fluctuation increases in the region around the $q = 3$ surface with the application of RMP was also being observed.

The experiments reported were carried out in lower single null KSTAR plasmas ($B_T = 1.6$ T, $I_p = 0.5$ MA, $n_e = 3.0$–4.0×10^{19} $m-3$, $R_0 = 1.8$ m, $R_{\mathrm{sep}} = 2.23$ m). The RMP coil current was set for $n = 1$ in the upper coil ($++--$) with 2.40 kAt, $n = 1$ in the middle coil ($-++-$) with 2.52 kAt, and $n = 1$ in the lower coil ($--++$) with 2.46 kAt. Measurements of v_ϕ of C^{+6} using charge exchange spectroscopy [14] are shown in Fig. 1. Figure 1(a) shows the v_ϕ evolution with time at different spatial positions for shot 10 884. From top to bottom, the positions of the v_ϕ are at normalized radial positions $\rho = 0.43$, 0.7, 0.87, 0.92, 0.96. Figure 1(b) shows the spectrum of the Mirnov signal. There is a clear magneto-hydrodynamics (MHD) mode with a frequency of about 8–11 kHz from 9 to 11 s. Figure 1(c) shows the time traces of the RMP coil current and the SMBI. The frequency of the SMBI modulation is 5 Hz, with a pulse duration of 6 ms. The SMBI plenum gas pressure is 0.8 MPa. The MHD mode frequency and the magnitude of v_ϕ both decrease after the SMBI pulse is injected, and then slowly recover.

With multiple V_ϕ perturbations measured, as shown in Fig. 1, we applied the perturbation transport analysis method [13] based on Fourier transform of the $V_\phi(t)$ at each minor radius and the propagation characteristics of perturbed V_ϕ can be extracted, which is shown in Fig. 2. Figure 2(a) shows the safety factor (H) profile, which is important for determining the resonant location of the RMP. The phase profile of the perturbed v_ϕ obtained is shown in Fig. 2(b) where the SMBI modulation is used as the phase reference. We emphasize that there are two phase minima—one at $q = 2$ located at $\rho = 0.42$ and another at $q = 3$, located at $\rho = 0.7$, as seen in Fig. 2(b). In perturbative plasma transport experiments, a minimum phase position generally indicates the position of an induced perturbation source [13,15]. The induced minimum phase in v_ϕ is unlikely to be due to a modulation of the "neutral particle source" because SMBI neutral particles cannot penetrate through the edge plasma to reach the $q = 3$ position, let alone $q = 2$ positions in KSTAR H-mode discharges [12]. Thus, the perturbation source in the plasma, corresponding to the minimum phase location, must be induced by a difference in plasma response due to the static RMP field with and without the edge SMBI perturbation. This is also consistent with the modulations in MHD mode frequency in corresponding to the SMBI directly as shown in Fig. 1(b). Comparing Figs. 2(a) and 2(b), we see that the phase minima are close to the $q = 3$ and $q = 2$ rotational surfaces, as shown by the red bars. The phase difference ($\Delta\phi$) ~0.11 rad, denoted by the vertical arrows in Fig. 2(b), between two locations at $q = 3$–$q = 2$ indicates the propagation delay associated with a first responses at the $q = 3$ surface, followed by the response at the $q = 2$ rational surface. This indicates that there is a time delay of the effect of the RMP field on the transport from $q = 3$ to $q = 2$. These experimental results

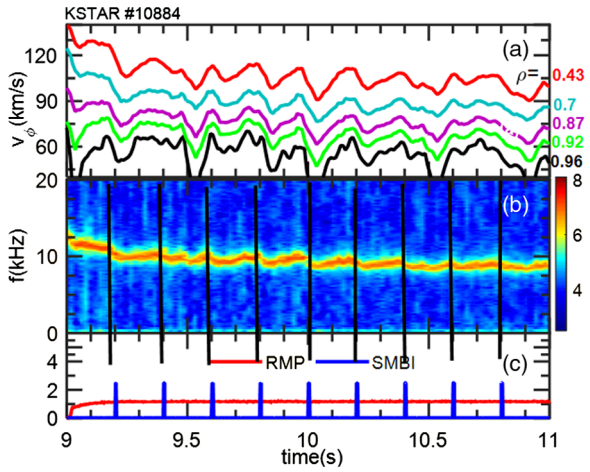

FIG. 1. (a) V_ϕ is modulated by small edge perturbations from the SMBI during the steady state RMP phase. (b) Spectrum of the Mirnov signal in arbitrary units. (c) Red curve is the current control signal of three RMP coils with ~2.4 kA and the blue pulses are the SMBI control signal.

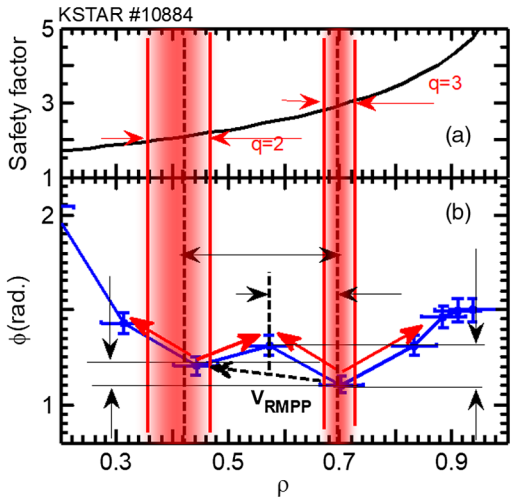

FIG. 2. (a) Safety factor profile and (b) phase profile of the perturbed V_ϕ. Vertical double red lines and red bars represent the uncertainties of the safety factor profiles and the minimum phase locations, respectively. The dashed lines indicate the locations of the $q = 3$ and $q = 2$ rational surfaces separated by 13 cm.

support the current RMP physics hypothesis being used for ITER, which states: "The RMP coils are shown to induce a layer of stochastic magnetic fields near the last resonant magnetic surface, typically $q = 3$ in the tokamak" [16].

Although no phase minima are observed when the modulated SMBI is applied without RMP in KSTAR H-mode plasmas, there is a uniform reduction in the rotation profile due to the edge localized drag from the SMBI [12]. Thus the presence of the RMP field in plasma and the presence of a phase minima in the plasma response to RMP can be uniquely determined by using small edge perturbation caused by SMBI pulses. As expected from our guiding idea envisioned for the experiment we measured a clear first response originating on the $q = 3$ surface, which we presumed is the location near the zero crossing of the perpendicular electron rotation frequency [17]. In addition, we saw a radial propagation of the changing rotation from the $q = 3$ point of origin both inward and outward with a subsequent change in the rotation profile at $q = 2$ as shown in Fig 2. Our physics hypothesis for this change in the RMP field originating at the $q = 3$ and shortly afterwards at $q = 2$ surfaces is that the SMBI creates a drag on the plasma as well as a change in the edge pressure gradient. The scenario envisioned here is that the drag from the SMBI pulses causes a change in the electron poloidal EXB and diamagnetic flow near the $q = 3$ rational surface which reduces the resonant field screening and allows a larger magnetic island to form. The larger $q = 3$ magnetic island causes an additional drag on the poloidal flow [17] which subsequently results in a reduction of the resonant screening on the $q = 2$ surface. We described our physics conclusion as a hypothesis since there is no a direct measurement of an increase in the magnetic island size on the $q = 3$ surface or the $q = 2$ surface. We prefer to remain conservative on this point until we can make a direct measurement of the changes in the islands on the $q = 3$ and 2 surfaces. We hope to be able to extend our results in the future on KSTAR by making measurements in the $q = 3$ and $q = 2$ islands using the electron cyclotron emission diagnostic to observe the T_e flattening and phase inversion associated with these magnetic islands.

A time delay for the propagation of the RMP resonance to move from the $q = 3$–$q = 2$ surfaces, given by $\Delta t = \Delta\phi/\omega = \Delta\phi/(2\pi f)$ Hz^{-1}, can be calculated using the $\Delta\phi$ and the f. Here, f is the modulation frequency of the SMBI (5 Hz) and $\Delta\phi$ is the phase delay of the RMP propagation from the $q = 3$ to $q = 2$ surfaces, which is 0.11 rad corresponding to $\Delta t = 4 \times 10^{-3}$ s. Thus, Δt is about 4 ms. This experimental result is in agreement with a modeling study result presented in [18] where the estimated RMP propagation time is shown to be on the milliseconds time scale. The radial midplane distance from the rational surfaces q=3–$q = 2$ is $\Delta\rho\times(R_{\rm sep}-R_0) \sim 0.3\times(R_{\rm sep}-R_0)=$ 0.13m. Then, the radial averaged velocity of the $V_{\rm RMPP}$ in H-mode plasma may be obtained using the distance and the time delay. $V_{\rm RMPP}$ is shown in Fig. 2 by the black dashed arrow with an inward propagation velocity of 32.5 m/s. The change in the toroidal phase response velocity of the perturbation V_ϕ is calculated in a similar way. One can define the $V_{\phi p}$ using $\Delta r/\Delta t$. Here, the Δr is about $0.15 \times (R_{\rm sep}\text{-}R_0) = 0.06$ m and Δt is $\Delta\phi/(2\pi f)$ Hz^{-1} $\sim 0.22/(2\pi 5)$ Hz$^{-1} = 7 \times 10^{-3}$ s, as shown in Fig. 2(b) where Δt is the time needed for the V_ϕ disturbance to propagate. Thus, the $V_{\phi p}$ is about 7.1 m/s from the $q = 3$ resonant surface to the point approximately half way between the $q = 2$ and $q = 3$ resonant surfaces, as shown in Fig. 2(b) by the red arrow. This indicates that the momentum transport of the perturbation V_ϕ is induced by the small perturbation of the SMBI when the RMP field is present. We note that $V_{\rm RMPP}$ is faster than the $V_{\phi p}$ in the region of $q = 3$–$q = 2$ rational surfaces. The ion sound speed, c_s, can be calculated using the $c_s = 9.79 \times 10^5 (\gamma Z K T_e/\mu)^{1/2}$ with $\gamma = 2$, $Z = 2$, $\mu = m_i/m_e = 2$, and $T_e = 1$ keV, then $c_s \sim 1.4 \times 10^3$ m/s. Thus, $V_{\rm RMPP}$ is about 2 orders of magnitude lower than the ion sound speed. It is also much slower that the Alfven speed indicating (2.9×10^5 m/s) that it may be associated with a change in the neoclassical toroidal viscosity torque [19] when the SMBI is applied. Here, the Alfven speed is $V_A = 2.18 \times 10^{11}\, \mu^{-1/2} n_i^{-1/2} B_t$ with $\gamma = 2$, $n_i = 6 \times 10^{13}$ cm^{-3}, and $B_t = 1.5 \times 10^4$ Gauss.

The temporal evolution of the toroidal rotation when the RMP field is presented, as shown in Fig. 3(a). The results show how the rotation profile changes as a function of time following the application of the RMP field and demonstrates the importance of the RMP fields on the $q = 3$ rational surface. In Fig. 3(b), $V_\phi(0)$ is an averaged profile of the toroidal rotation just before the RMP is applied from 8.9 to 9.0 s, and the $V_\phi(t)$ is the toroidal rotation profile at different times with RMP. The $q = 3$ rational surface and the pedestal top are denoted by black and red horizontal dashed lines, respectively. It can be clearly seen in Fig. 3(a) that the braking in V_ϕ occurs strongly around the $q = 3$ rational surface for all the time after the application of RMP starting from $t = 9.0$ s, although the braking is further enhanced and transiently spreads inward and outward following the SMBI pulse at $t = 9.2$ s. A more detailed analysis of the induced V_ϕ braking by the RMP field is shown in Fig. 3(b). The black curve is the V_ϕ profile without RMP at $t = 8.9$ s, the red curve is with the RMP at $t = 9.15$ s, and the blue curve is the difference between the black and the red curves (multiplied by a factor of 8). Figure 3(b) clearly shows that the largest change in V_ϕ occurs at $\rho = 0.7$, which corresponds to the location of the $q = 3$ rational surface, showing that the V_ϕ braking occurs around the $q = 3$ rational surface, as shown in Fig. 3(b) by the red arrow. This V_ϕ braking induces the propagation of the toroidal momentum inward and outward from the

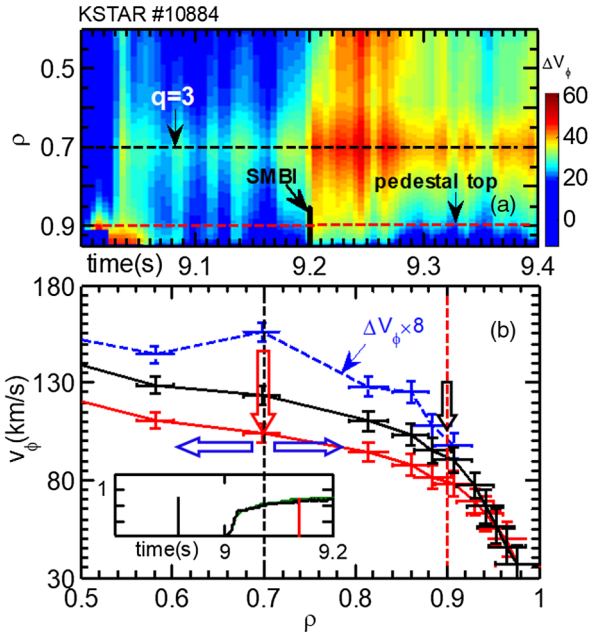

FIG. 3. (a) ΔV_ϕ (in km/s) as a function of time following the application of the RMP field. (b) V_ϕ profiles without and with RMP for shot 10 884 as shown using the black curve and the red curve, respectively. The ΔV_ϕ is shown as blue dashed line. The inner small box represents the RMP time trace, and the black and red vertical lines in the small box indicate the time points of the V_ϕ profiles obtained at 8.9 and 9.15 s, respectively.

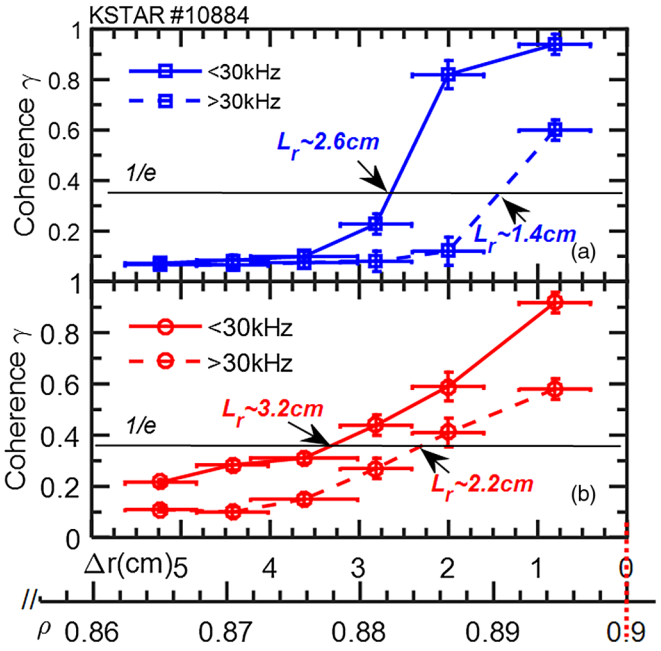

FIG. 4. (a) Coherence coefficient (γ) profiles and radial correlation length (L_r) without RMP during 9.0–9.006 s and (b) the same as in (a) but with RMP during 9.7–9.706 s. No SMBI pulses were injected during the time windows. The position of the pedestal top is at $\rho = 0.9$, as shown by the red dotted line.

resonant location, as shown in Fig. 3(b) by the blue arrows. We emphasize again that the presence of RMP is required for the localized braking as shown in Fig. 3. In contrast, without RMP, applying SMBI only led to a uniform reduction in toroidal rotation (not a localized V_ϕ braking around the rational surface) [12].

In addition to braking toroidal rotation, RMP may also induce changes in plasma turbulence and thus local transport. Here, we compare the radial density fluctuation profiles with and without RMP using the 4×16 beam emission spectroscopy (BES) arrays in KSTAR [20]. The analysis range of the BES measurements in the experiments is from -5.1 to -13.8 cm below the midplane and from the separatrix to a distance 12 cm inside of the plasma. The radial correlation length of the density fluctuation with and without the RMP was obtained using BES for shot 10 884, as shown in Fig. 4. Here, the $1/e$ coherence value is designated as the radial correlation length (L_r) [21]. The measurement radial range is inward beginning from the pedestal top, which is the reference point located at the pedestal top for the coherence (γ). With the RMP, L_r increases from 1.4 to 2.2 cm for fluctuations with $f >$ 30 kHz (denoted ambient turbulence, AT) and increases from 2.6 to 3.2 cm for fluctuations with $f < 30$ kHz (denoted low frequency turbulence, LFT), as shown in Figs. 4(a) and 4(b), respectively. In order to avoid the influence of the SMBI injection on the turbulence analysis, two special time windows for turbulence analysis were chosen: the time window without RMP is from 9.0 to 9.006 s, and the time window with RMP is from 9.7 to 9.706 s, which is far from the SMBI injection time. This means that there are no SMBI pulses during the time windows of the turbulence analysis. This shows that the density fluctuation radial scale length increases with application of a steady state RMP for both the LFT and the AT. This is consistent with the turbulence causing additional radial transport during the RMP [22]. The increased turbulence and V_ϕ braking produced by the RMP result in the reduced height of the pedestal toroidal rotation [Fig. 3(b) by the black arrow].

In conclusion, we report the first investigations of the propagation dynamics of resonant magnetic perturbations fields in KSTAR H-mode plasmas using injection of small edge perturbations produced by a supersonic molecular beam injection system. The experiments demonstrate that the RMP penetrates the pedestal region where it first resonates at the $q = 3$ rational surface and then at the $q = 2$ rational surface. From the $q = 3$ rational surface to $q = 2$ rational surface, the radial averaged velocity of the RMP penetration (V_{RMPP}) in the H-mode plasma is about 32.5 m/s; that is much slower than either the ion sound or Alfven velocity but more than 4 times faster than the radial propagation of the change in the toroidal rotation. The RMP field resonates at the rational surface, brakes the toroidal velocity V_ϕ, induces the propagation of the toroidal momentum inward and outward from the resonant location,

increases the density fluctuation, and finally results in the reduced height of the pedestal toroidal rotation. These new results provide further physical insight needed to refine our knowledge related to the physics of RMP propagation dynamics and the ELM control using RMP in *H*-mode plasmas, and the results extend the current understanding of the RMP physics required for developing reliable ELM control in ITER.

This work was supported in part by the U.S. Department of Energy under DE-FG02-08ER54999, DE-FC02-04ER54698 De-FG03-97ER54415, DE-FG02-89ER53296, DE-FG02-07ER54917, DE-FG02-07ER54917, DE-AC02-09CH11466, DE-SC0001961, a 2016–17 General Atomics contract from the National Fusion Research Institute.

[1] S. Wiggins, *Chaotic Transport in Dynamical Systems*, Interdisciplinary Applied Mathematics Vol. 2, (Springer, New York, 1992).
[2] J. D. Meiss, Rev. Mod. Phys. **64** (1992).
[3] J. M. Ottino, *The Kinematics of Mixing: Stretching, Chaos, and Transport* (Cambridge University Press, Cambridge, England, 1989).
[4] B. J. Albright, Phys. Plasmas **6**, 4222 (1999).
[5] A. B. Rechester and M. N. Rosenbluth, Phys. Rev. Lett. **40**, 38 (1978).
[6] T. E. Evans *et al.*, Phys. Rev. Lett. **92**, 235003 (2004).
[7] A. Loarte *et al.*, Plasma Phys. Controlled Fusion **45**, 1549 (2003).
[8] M. F. Heyn, I. B. Ivanov, S. V. Kasilov, and W. Kernbichler, Nucl. Fusion **46**, S159 (2006).
[9] M. F. Heyn *et al.*, *Problems of Atomic Science and Technology*, Plasma Physics Series 1 (North Holland, Amsterdam, 2013), Vol. 83, p. 51.
[10] A. Kirk *et al.*, Nucl. Fusion **50**, 034008 (2010).
[11] W. W. Xiao, T. E. Evans, G. R. Tynan, and D. Eldon, Nucl. Fusion **56**, 064001 (2016).
[12] W. W. Xiao *et al.*, Nucl. Fusion **54**, 023003 (2014).
[13] N. J. Lopes Cardozo, Plasma Phys. Controlled Fusion **37**, 799 (1995).
[14] W. H. Ko, H. Lee, D. Seo, and M. Kwon, Rev. Sci. Instrum. **81**, 10D740 (2010).
[15] W. W. Xiao *et al.*, Phys. Rev. Lett. **104**, 215001 (2010).
[16] C. Horton and S. Benkadda, *ITER Physics*, (World Scientific Publishing Co. Pet. Ltd, Singapore, 2015), Chap. 6, p. 156.
[17] N. M. Ferraro, T. E. Evans, L. L. Lao, R. A. Moyer, R. Nazikian, D. M. Orlov, M. W. Shafer, E. A. Unterberg, M. R. Wade, and A. Wingen, Nucl. Fusion **53**, 073042 (2013).
[18] Y. Q. Liu, A. Kirk, and Y. Sun, Phys. Plasmas **20**, 042503 (2013).
[19] K. C. Shaing, Phys. Plasmas **10**, 1443 (2003).
[20] Y. U. Nam, S. Zoletnik, M. Lampert, and Á. Kovácsik, Rev. Sci. Instrum. **83**, 10D531 (2012).
[21] J. Schirmer, G. D. Conway, E. Holzhauer, W. Suttrop, H. Zohm, and the ASDEX Upgrade Team, Plasma Phys. Controlled Fusion **49**, 1019 (2007).
[22] G. R. Mckee *et al.*, Nucl. Fusion **53**, 113011 (2013).